Journal of Asian Ceramic Societies 3 (2015) 50–58

HOSTED BY

Contents lists available at ScienceDirect

Journal of Asian Ceramic Societies

journal homepage: www.elsevier.com/locate/jascer

Mineralogical and physicochemical characterization of Ngaye alluvial clays (Northern Cameroon) and assessment of its suitability in ceramic production

Soureiyatou Fadil-Djenabou[a], Paul-Désiré Ndjigui[a], Jean Aimé Mbey[b,c,*]

[a] Department of Earth Sciences, University of Yaoundé 1, P.O. Box 812, Yaoundé, Cameroon
[b] Department of Inorganic Chemistry, University of Yaoundé 1, P.O. Box 812, Yaoundé, Cameroon
[c] Laboratoire Interdisciplinaire des Environnements Continentaux, Université de Lorraine, UMR 7360, 15 Avenue du Charmois, B.P. 40, F-54501 Vandoeuvre-lès-Nancy Cedex, France

ARTICLE INFO

Article history:
Received 2 September 2014
Received in revised form 14 October 2014
Accepted 23 October 2014
Available online 11 November 2014

Keywords:
Mineralogy
Physicochemistry
Alluvia
Clays
Ceramic

ABSTRACT

This study reports the physicochemical analysis of three alluvial clastic clays from the Ngaye River in northern Cameroon. X-ray diffraction, infra-red spectroscopy, scanning electron microscopy and thermal analysis are used to establish the mineralogical composition. It is found that the main clay minerals in these samples are kaolinite, muscovite-illite and smectite associated with quartz, goethite, feldspars and anatase. This mineralogical assemblage is in accordance with the chemical analysis which further confirmed the high quartz proportion. The low content in fluxing agent is indicated by the low contents in Na_2O, K_2O, MgO and CaO. The low content in fluxing agent and high sand proportion result in poor vitrification in ceramic testing brick obtained at 900 °C, 1000 °C and 1100 °C. For all the firing temperatures, linear shrinkage varied from 0.7% to 2.6%, weight loss varied from 3.5% to 7%, bulk density varied from 1.6 to 1.8 g/m^3, water absorption decreased from 20.7% to 12.7%, and flexural strength (σ) varied from 0.60 to 2.07 MPa.

The Ngaye alluvial clastic clays could be used in the fabrication of bricks (commons and perforated). However, an increase of fluxing agent and clays is needed to improve the mechanical performance of the ceramic products.

1. Introduction

Clays are raw materials of interest in ceramic building materials due to their thermal conductivity and strength [1,2]. They can be used in many other industrial applications such as paper, paint, rubber and plastics, insecticides, formulation of additives for food, cosmetics, pharmaceutics, drilling fluids, fertilizer carriers, and geochemical barriers [3–10]. The use of clay materials in a giving industry is mainly due to their mineralogical and physicochemical properties, which depend on their structure and composition [10]. In Cameroon, the valorization of clay materials is a domain of growing interest. The actual domains of interest are geopolymer applications [11,12], nanocomposite material [13,14] and ceramic applications [15,16]. Ngaye region is made up of vast alluvial plains with abundant clay materials in their numerous valleys. Despite its high proportion, clay materials from Ngaye are only exploited for traditional pottery and local ceramic bricks. This is primarily because the potentialities of these clays are not evaluated. To date, no study that evaluates the potential applications of these materials is reported. It is then obvious that their mineralogical, chemical and physical properties need to be analyzed in order to ameliorate their use in ceramic products and to open ways for other potential industrial applications. Thus, this paper aims to contribute to the study of mineralogical and physicochemical properties of Ngaye alluvial clays and to analyze their suitability in ceramic making.

2. Geographical and geological setting

Ngaye region is situated between 7°13′ and 7°14′N, and 15°26′ and 15°28′E, South of Touboro Sub-division and Mayo Rey Division, in the North Region. It is found in the North of Adamawa, a few kilometers to the border with the Central African Republic (Fig. 1). This region is characterized by a humid sudanian climate, and a

* Corresponding author at: Department of Inorganic Chemistry, University of Yaoundé 1, P.O. Box 812, Yaoundé, Cameroon. Tel.: +237 99 23 89 25.
E-mail addresses: soureiyatou@yahoo.fr (S. Fadil-Djenabou), lndjigui@yahoo.fr (P.-D. Ndjigui), mbey25@yahoo.fr (J.A. Mbey).
Peer review under responsibility of The Ceramic Society of Japan and the Korean Ceramic Society.

2187-0764
http://dx.doi.org/10.1016/j.jascer.2014.10.008

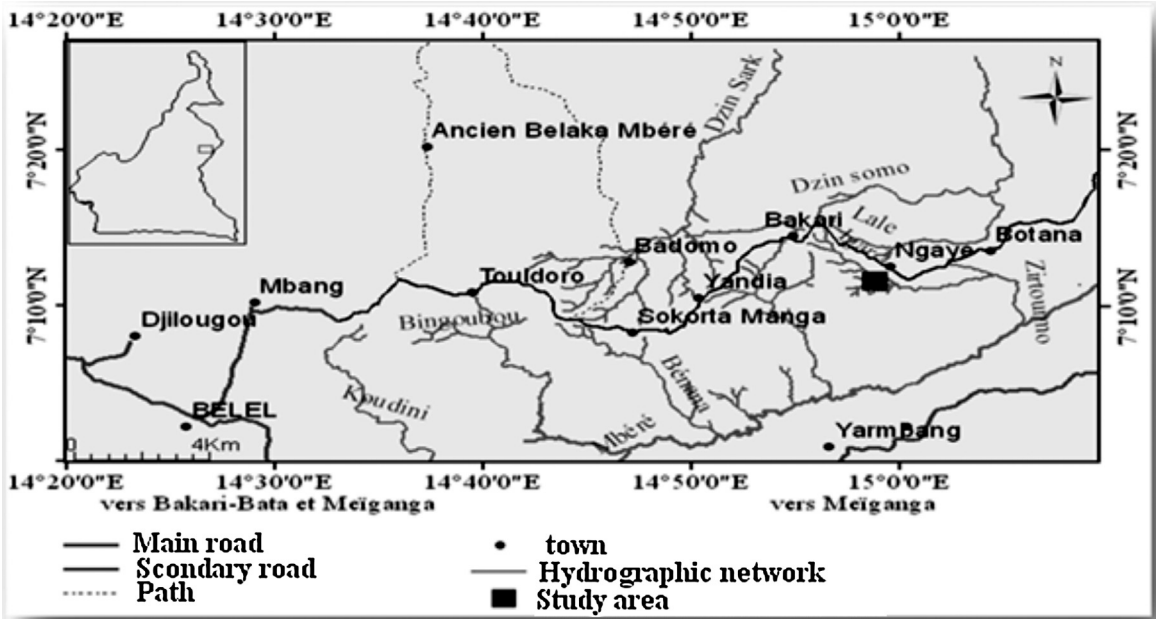

Fig. 1. Location map of the study area.

dendritic drainage pattern along the Ngaye River. The relief is very varied despite the predominance of plains [17]. The Ngaye region is made up of succession of hills separated by small valleys with eroded or gullied bell-shaped bottoms [18]. It is also characterized by a relatively accidental relief composed of a set of massifs locally called "Ngao", whose altitudes vary from 400 to 1300 m [18]. These "Ngaos" are separated by more or less vast plains [19]. The geomorphology of Mayo Rey can be subdivided into three distinct zones. In the North of Mayo Rey, vast plains and wide valleys dominated by the Goumbayré hills are observed; at the center, a series of more or less vast erected massifs of unequal altitudes; in the South, the areas of Meiganga-Tignère and the Vina valley are characterized by low lands and projecting reliefs [17]. The Ngaye's village, situated in the Mbere valley with altitudes between 650 and 1000 m, is constituted of symmetric hills with rounded summits, residual buttes in a horse back form and very vast alluvial plains. Along rivers, vast plains with large alluvial terraces are observed. Geologically, the following rocks are observed in Mayo Rey [20,21]: sedimentary rocks such as sandstones and marl of Cretaceous age at Ngoumi; plutonic rocks such as granites and syenites of Cambro-Ordovician age (570–440 Ma). Ancient and discordant syntectonic granites, syenites, diorites and gabbros associated to the basement complex which covers a large part of southern Touboro and metamorphic rocks such as mica schists, gneisses, anatexis or oriented granites associated to the basement complex cover a large part of the region as well as the study area.

3. Materials and methods

3.1. Samples and sampling techniques

Three bulk samples were collected from three layers in a vertical section of the Ngaye River terrace. The samples were designated MD10 for the bottom layer, MD20 for the middle layer and MD30 for the upper layer [18].

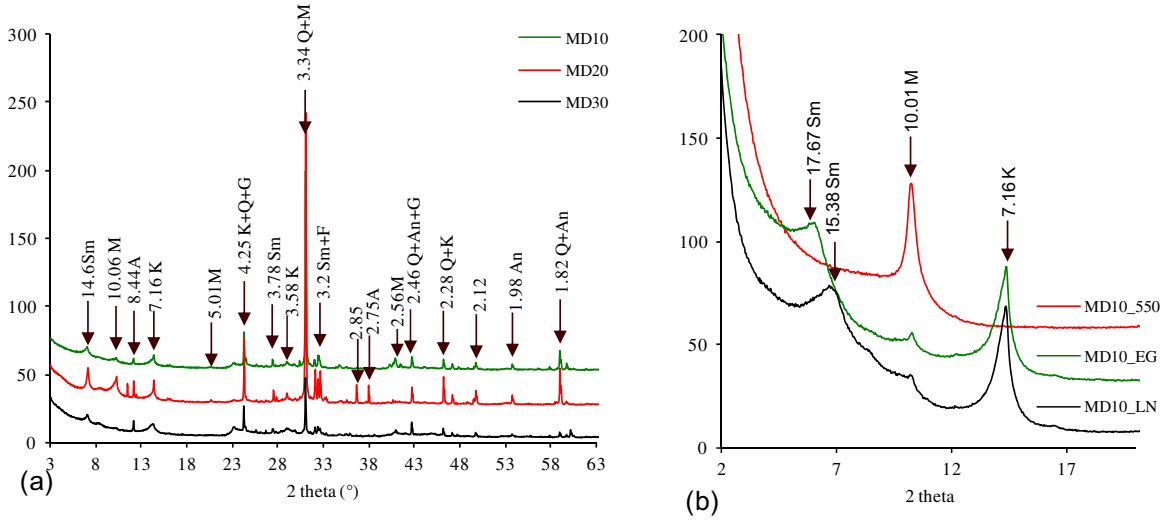

Fig. 2. XRD patterns of the samples: (a) random, (b) examples for sample MD10 of: orientated (MD10_LN); oriented and glycolated (MD10_EG) and heated at 550 °C (MD10_550). Sm = smectite; M = muscovite; K = kaolinite; Q = quartz; F = feldspar; G: goethite; A = amphibole; An = anatase.

3.2. Analytical techniques

Particle size distribution (PSD) was obtained by sieving for the coarse and fine sand fractions using sieves of 200 and 50 μm respectively. The silt- and clay-sized fractions were obtained by sedimentometry using Robinson's pipette method. Colors of raw samples were determined using the Munsell Soil Color Book. Atterberg's Consistency liquid limit (LL) and plastic limit (PL) were measured using the Casagrande apparatus [22]; plasticity index (PI) was calculated as follows:

$$PI = LL - PL \quad (1)$$

The mineralogical composition was determined by X-ray diffraction (XRD) analysis using a D8 Advanced Bruker Diffractometer equipped with a Co Kα radiation (λ = 1.7890 Å) operating at 35 kV and 45 mA. The diffraction patterns were obtained from 1.5 °C to 32 °C at a scanning rate of 1° min^{-1}. Infra-red spectra were recorded in diffuse reflectance mode using a Bruker Fourier Transform Interferometer IFS 55. The spectra, recorded from 4000 cm^{-1} to 600 cm^{-1} with a resolution of 4 cm^{-1}, are obtained by accumulation of 200 scans. Scanning electron microscopy (SEM) coupled to energy dispersive X-ray spectroscopy (EDS) was carried out on a Hitachi S-4800 using a YAG (Yttrium Aluminium Garnet) backscattered secondary electron detector. For SEM analysis, the powdered samples are carbon coated prior to the analysis.

Thermal analysis was performed on a homemade Controlled Rate Thermal Analysis (CRTA) apparatus. In CRTA, the temperature increase is controlled by the reaction rate through pressure measurement. The sample is placed under dynamic vacuum through a micro-leak which is calibrated to emit quantified gases. The limiting pressure is fixed at 2 Pa, which ensures a linear weight loss with respect to time [23]. For analysis, samples of about 50 mg were heated from ambient temperature (23 °C) to 800 °C. The concentrations of major elements were determined using X-ray fluorescence (XRF) after being heated and melted with a flux of lithium tetraborate and analyzed using a Pan Analytical Axios Advanced PW4400.

Technological properties were determined on test briquettes (80 mm × 40 mm × 10.4 mm) obtained by compressing humidified crushed clayey material with a SPECAC laboratory hydraulic press of 10 tons. The added water, for humidification, was in a weight percentage of 10–15%, with respect to the clay material. The briquette specimens were placed on a wooden board for 24 h for air drying, followed by oven drying at 105 °C for 24 h to eliminate adsorbed water. After oven drying, the specimens were fired in a Nobertherm programmable electric furnace at 900 °C, 1000 °C and 1100 °C. The firing profile was as follows: 4 °C/min from 23 °C up to 580 °C and 5 °C/min from 580 °C up to the final temperature. Each sample is left to equilibrate for 2 h at 580 °C, before the following heating sequence. After soaking for 30 min at each final temperature, the specimens were furnace-cooled to room temperature. Color of fired briquettes was appreciated in the same way as raw samples. Sound test was done by knocking the fired briquettes with a metal rod. The densification parameters of the fired briquettes were accessed by measuring linear shrinkage, weight loss, water absorption capacity and bulk density (obtained after the ASTM C20-00 norm). The flexural strength was obtained by a three-point bending method according to the ASTM C674-77 norm.

Linear shrinkage (LS) was determined by measuring the length of the briquettes before firing (L_0) and after firing (L). LS was calculated as

$$LS(\%) = [(L_0 - L)/L_0] \times 100 \quad (2)$$

Weight loss (WL) was calculated between 105 °C and peak firing temperatures (900 °C, 1000 °C and 1100 °C) using the following formula:

$$WL(\%) = [(Md - Mf)/Md] \times 100 \quad (3)$$

where Md is the dry mass (105 °C) and Mf is the fired mass (at each final firing temperature).

Bulk density (B) of a briquette is obtained as the ratio of the fired briquette mass to the measured volume of the briquette (Eq. (4) below):

$$B(g/cm^3) = Mf/V \quad (4)$$

V is volume of fired briquette.

Water absorption capacity was calculated according to Eq. (5):

$$WA(\%) = [(W - Mf)/Mf] \times 100 \quad (5)$$

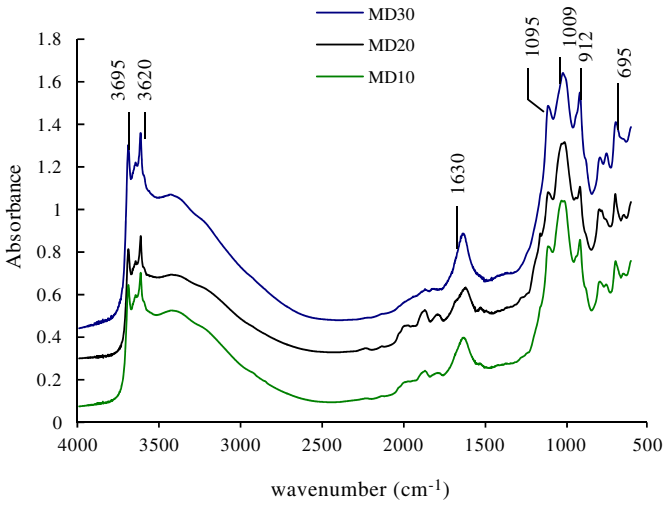

Fig. 3. FTIR spectrum of Ngaye alluvial clays.

Table 1
Physical properties and chemical composition of Ngaye clays.

	MD10	MD20	MD30
Physical properties			
Samples colors[a]	Dark yellowish brown	Yellowish brown	Dark gray
Particle size distribution (%)			
Clay (<2 μm)	27.3	33.9	43.2
Silt (2–50 μm)	16.5	8.2	0.83
Sand (>50 μm)	55.9	57.8	55.5
Atterberg limits			
Liquid limit (LL)	32.6	57.3	50.7
Plastic limit (PL)	22.8	36.5	31.8
Plastic index (PI)	9.8	20.8	18.9
Chemical composition			
SiO_2	55.05	75.04	67.96
Al_2O_3	19.80	20.89	23.12
Fe_2O_3	7.161	6.25	6.56
MnO	0.07	0.04	0.05
MgO	1.21	0.85	0.64
CaO	1.04	1.07	0.83
Na_2O	0.92	1.08	0.73
K_2O	1.78	2.00	1.85
TiO_2	0.82	0.48	0.64
P_2O_5	0.07	0.04	0.06
LOI	11.16	3.87	7.50
Total	99.08	99.62	98.94

[a] The Munsell code for MD10, MD20 and MD30 samples are, respectively, 10YR4/3, 10YR5/4 and 10YR3/1.

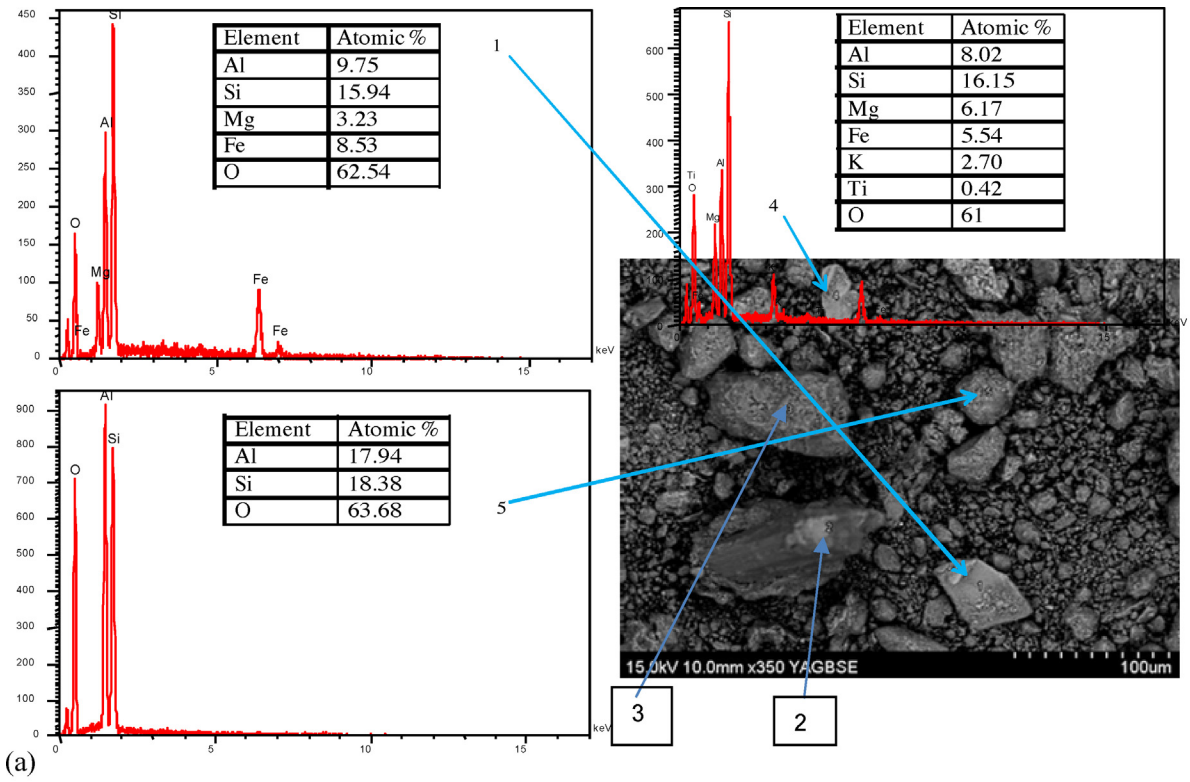

(a)

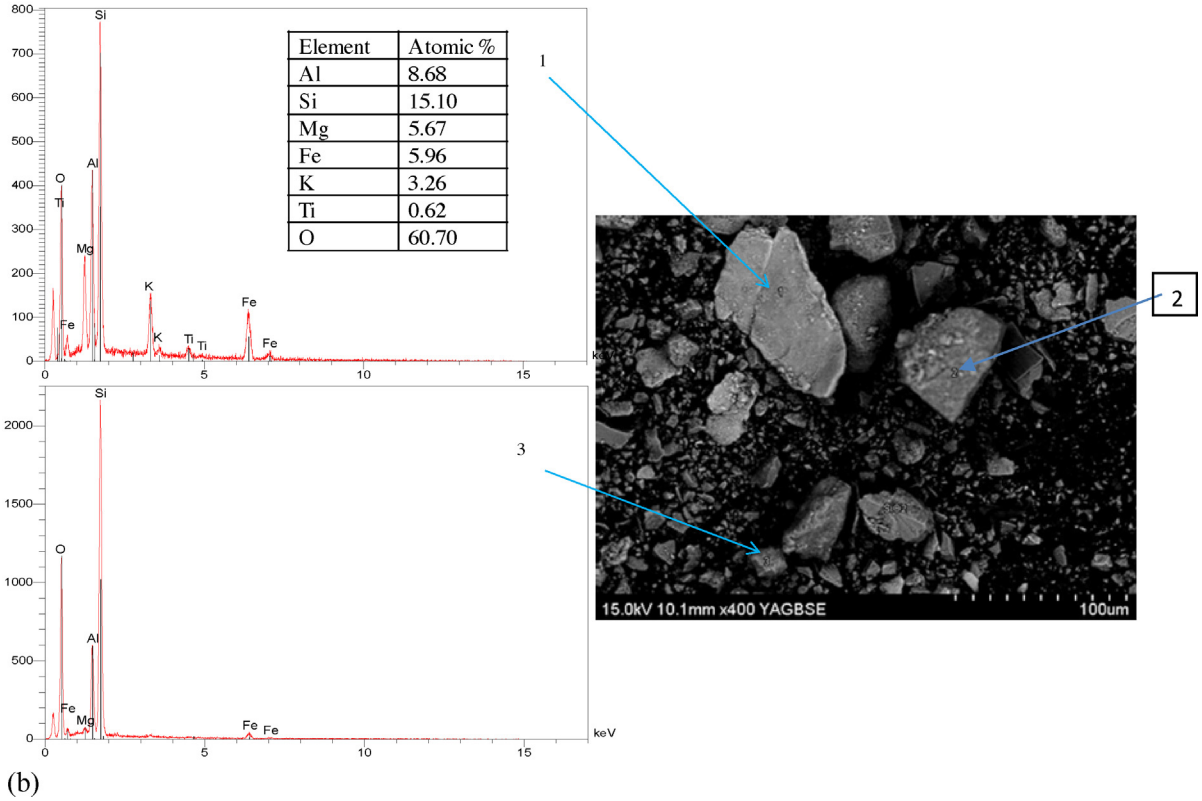

(b)

Fig. 4. SEM micrographs of raw material coupled with EDS spectrum of differents phases: (a) MD30, (b) MD20 and (c) MD10.

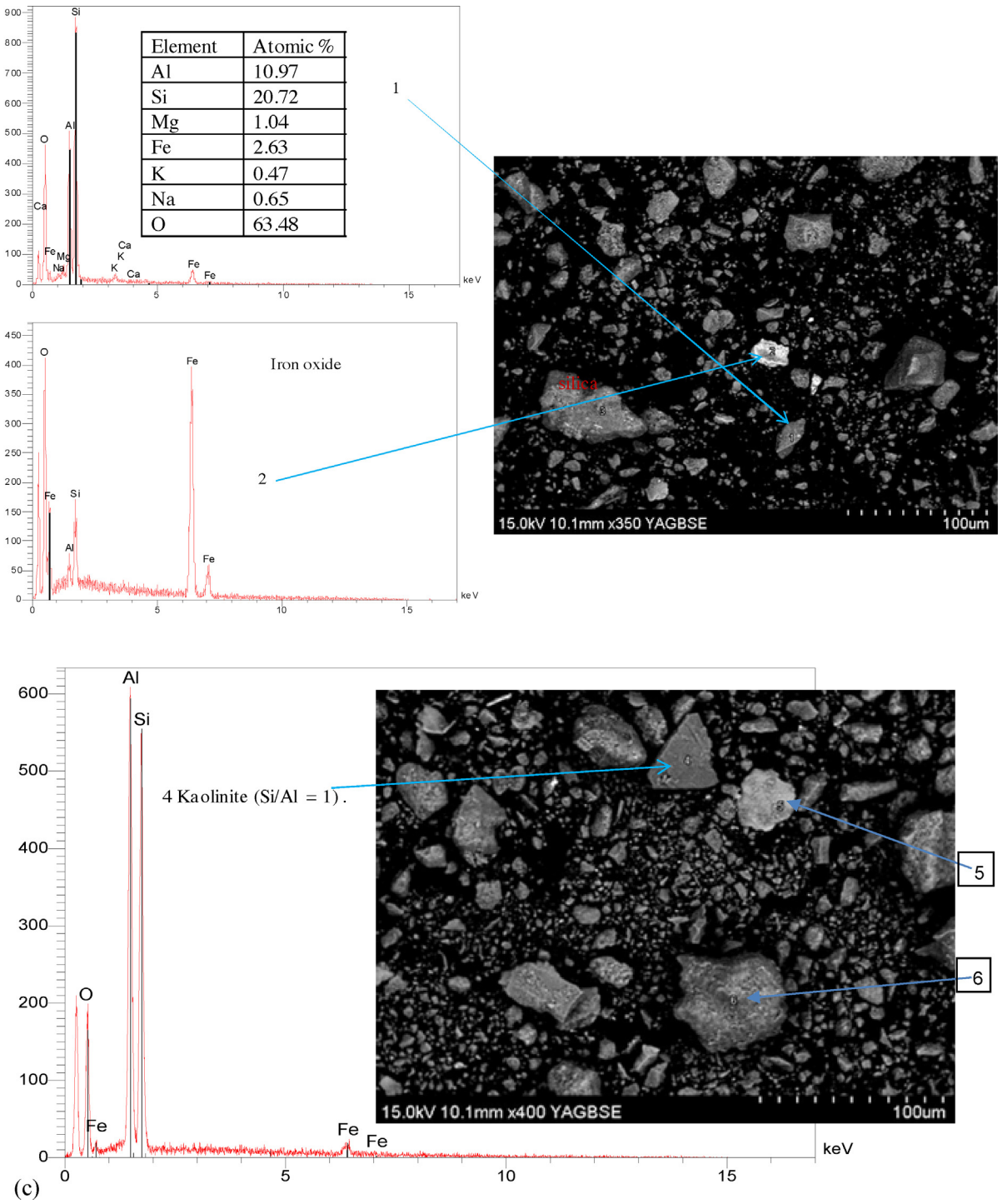

Fig. 4. (*Continued.*)

where W is the mass of wet briquette after 24 h soaking in water and Mf is the mass of the fired briquette.

Flexural strength (σ) of briquettes was evaluated using a three-point bending test. The flexural strength was calculated after Eq. (6):

$$\sigma = 3P \times L/2b \times d^2 \quad (6)$$

where P is the maximum load at rupture (N), L is the distance between the supporting knife edges (mm), b is the width of briquette (mm) and d is the thickness of briquette (mm).

4. Results and discussion

4.1. Mineralogical and physicochemical composition

From XRD patterns (Fig. 2), the mineral composition includes quartz, kaolinite, muscovite-illite and smectite associated to goethite, feldspars, amphibole and anatase (Fig. 2a). The oriented samples were analyzed to further confirm the nature of the clay phases in the samples. Because the three samples exhibit the same composition, an example of obtained patterns is given for sample MD10 in Fig. 2b. The glycerol solvatation clearly leads to the

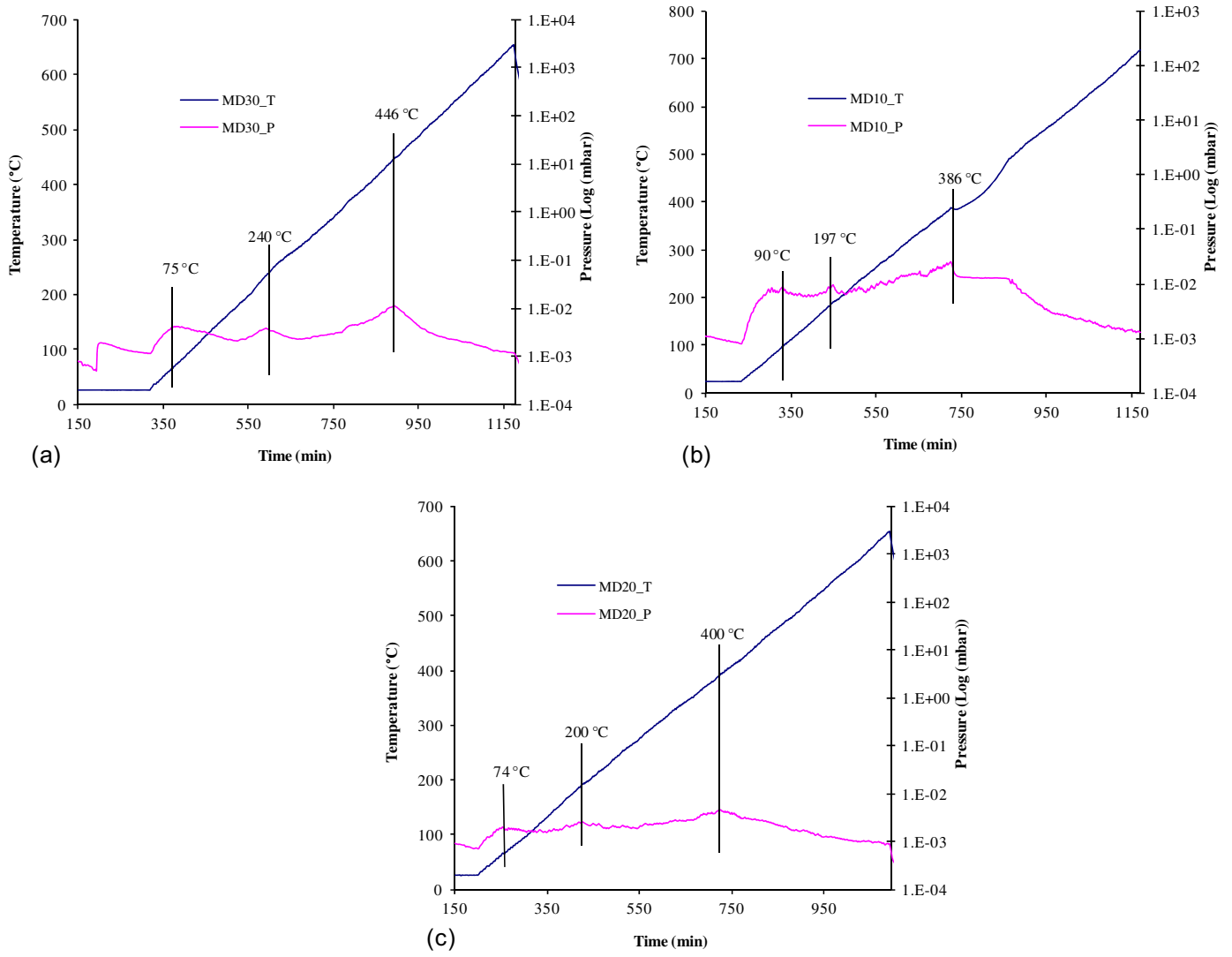

Fig. 5. Thermal analysis (CRTA) of the samples.

displacement of the diffraction peak at 15.38 Å to 17.67 Å, indicating the presence of smectite. The diffraction peaks at 10.01 Å and 7.16 Å are not displaced during glycolation and further confirm the presence of muscovite-illite and kaolinite. The 7.16 Å diffraction peak disappears after firing at 550 °C as expected while the 10.01 peak is still observable. The intensity increase of the 10.01 Å diffraction peak after thermal treatment at 550 °C is due to the collapse of the smectite diffraction peak at 10 Å which is an additional evidence of smectite. The FTIR spectra presented in Fig. 3 confirms the high content in kaolinite as shown by the quadruple bands at 3697 cm^{-1}, 3662 cm^{-1}, 3648 cm^{-1}, 3620 cm^{-1} corresponding to O–H stretching bands, usually observed in kaolinite based clay [24,25]. The Si–O stretching bands at 1095–1009 cm^{-1} [26], and the Al–O bending at 912 cm^{-1} are characteristic of aluminosilicate minerals. The stretching and bending of hydration water are observed at 1630 cm^{-1}.

The scanning electron microscope (SEM) observations coupled with EDS are presented in Fig. 4. The identified mineral using XRD are confirmed. In Fig. 4a the presence of kaolinite is shown by the Si/Al ratio of about 1 for point 5 which is similar in composition with points 2 and 3 (Fig. 4a). At point 1, the Si/Al ratio of 1.6 is related to muscovite-illite content. The elemental composition found at point 4 is characteristic of a mixture of smectite (Si/Al ratio is about 2) and titanium oxide. In Fig. 4b, the elemental composition of MD20 at point 1 and 2 is indicative of smectite due to the Si/Al ratio of 2. The presence of Mg is an additional evidence of the smectite in these phases. The presence of potassium is assumed to be due to the muscovite-illite content. Ti and Fe are indicative of their related mineral. From XRD and FTIR, the Fe and Ti based mineral are goethite and anatase. The EDS analysis of MD10 also confirms the presence of smectite (points 1, 5 and 6) and kaolinite (point 4) (Fig. 4c). Iron oxide (or hydroxyl) is observed at point 2 (Fig. 4c). The EDS analysis is in accordance with the mineral composition evidence from XRD and FTIR.

Thermal analysis using CRTA of the sample is presented (Fig. 5). For the three samples, three characteristic temperatures are observed. The first temperature (90 °C, 74 °C and 75 °C, respectively for MD10, MD20 and MD30) was assigned to the release of the hydration water; the second peak temperature (197 °C, 200 °C and 240 °C respectively for MD10, MD20 and MD30) is related to the conversion of goethite to hematite. The last peak (386 °C, 400 °C and 446 °C) is the dehydroxylation temperature of the clay minerals.

The chemical composition of the Ngaye alluvial clays (Table 1) indicates high amount of SiO_2 which is in accordance with the high content in quartz as shown by the XRD patterns. The Al_2O_3 contents are rather moderate and indicate low clay mineral proportion in these samples. The high proportion of quartz (free silica) is confirmed by the high SiO_2/Al_2O_3 ratio [27]. Sifting may be useful

to improve the clay content of the material prior to its use. The MgO content that can be associated to 2:1 clay is rather low (MgO, 1.21 wt.%; 0.84 wt.%; 0.64 wt.% respectively for MD10, MD20 and MD30) and it is an evidence that kaolinite is the main clay mineral in the Ngaye alluvial clays. The content of fluxing oxides (Na_2O, K_2O, CaO and MgO) is low and these may cause insufficient sintering during cooking (Table 1).

4.2. Particle size distribution

The particle size distribution is presented in Table 1. From these results, MD30 is sandy clays (43.2% clays, 0.83% silts and 55.5% sands), while MD20 and MD10 are sandy clays loam (27.3–33.9% clays, 8.2–16.5% silts and 55.9–57.8% sands). The importance of sand fraction is in accordance with XRD and chemical data (major elements) that indicate high quartz proportion. The clay fraction (<2 μm) that varies from 27.3% to 43.2% may cause difficulties in ceramics production. However, crushing and sifting can be used to reduce the content in coarse particle (>50 μm) and this may result in better ceramic products [28]. In the Winkler diagram of grain size classification of clay raw materials, MD20 and MD10 fall in the fields of vertically perforated bricks and common bricks respectively (Fig. 6), while MD30 does not fall in any defined zone of the Winkler diagram. The low silt proportion of MD30 probably accounts for this and addition of degreaser (increased silt content) is needed to facilitate the processing of this sample.

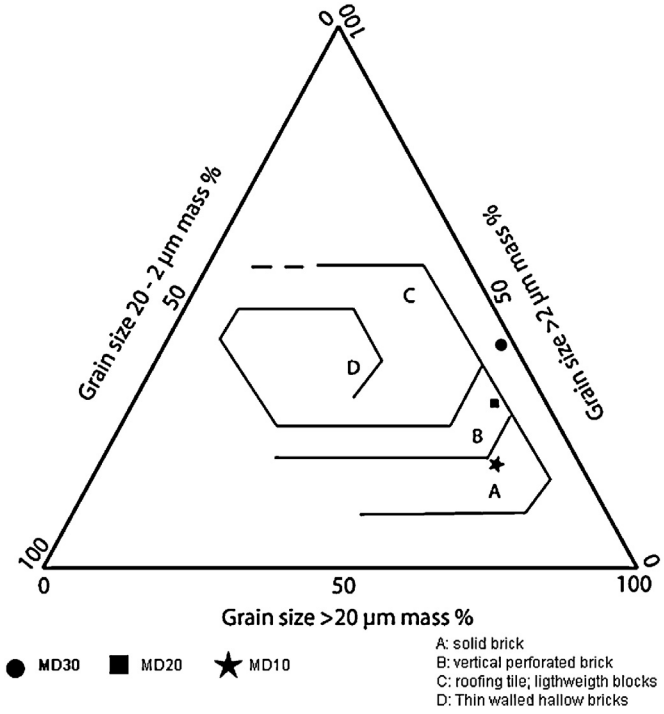

Fig. 6. Winkler diagram.

4.3. Atterberg's limits

The data of Atterberg's limits are presented in Table 1. The plasticity of the Ngaye alluvial clays is mostly influenced by the clay fraction. Hence, MD20 and MD30 with higher clay contents are more plastic than MD10 with less clay proportion. On the Casagrande chart (Fig. 7), MD20 and MD30 are comprised within the zone of high plastic organic clays and inorganic silt while MD10 is medium plastic clay. The plasticity is favorable for extrusion and manual processing but the proportion of silts and sands may affect the processability. This plasticity is consistent with the classification from the Winkler diagram and helps to confirm that the silt content of MD30 may explain its positioning in the Winkler diagram.

4.4. Properties of the fired products

The data of ceramic behavior are presented in Table 2. The sound of the Ngaye alluvial clays after firing from 900 °C to 1100 °C varied from dull to inferior metallic sound. This is principally due to poor sintering caused by low content in fluxing oxides and high content in sand [29].

Weight loss (Table 2) shows very little changes which can be attributed to the elimination of organic matter by combustion and water by dehydration during firing [30].

Bulk density of the fired samples shows low values which increase with temperature, except MD10 sample (Table 2). This is likely due to very little glassy phase formation consequence of low content in fluxing agents. Linear shrinkage was generally low and increased with firing temperature (Table 2). Hence at 900 °C the linear shrinkage is 1.4%, 0.5% and 1.3% for MD10, MD20 and MD30 respectively. In the same order, it slightly increased to 1.5%, 0.7% and 1.4% at 1000 °C; at 1100 °C significant changes were observed; the values increased to 2.6%, 1.3% and 1.6% respectively. The increase at 1100 °C is probably due to the starting of glassy phase formation. The flexural strength values ranged between 0.60 and 2.07 MPa, for all firing temperatures (Table 2). These low flexural strength values are probably due to poor sintering associated to low content in total melting feldspars associated to relatively low processing temperatures which are not favorable to sintering. Water absorption decreases with firing temperature (Table 2). This decrease is associated to glassy phase formation that penetrates into pores closing them and isolating neighboring pores. The decrease is more marked for samples fired at 1100 °C [10,31]. The water absorption at 1000 °C and 1100 °C is <20% indicating that the Ngaye alluvial clays can be used for brick and roofing tiles according to the Brazilian classification reported by Ngun et al. [31].

Table 2
Properties of the fired briquettes.

Samples	MD10			MD20			MD30		
Temperature (°C)	900	1000	1100	900	1000	1100	900	1000	1100
Color	Yellowish brown	Light brown	Reddish brown	Reddish brown	Reddish brown	Reddish brown	Reddish brown	Reddish brown	Reddish brown
Sound	Metallic	Metallic	Metallic	Dull	Dull	Dull	Dull	Dull	Dull
Linear shrinkage (%)	1.43	1.54	2.59	0.51	0.74	1.32	1.32	1.42	1.62
Weight loss (%)	6.80	6.90	7.02	3.51	3.59	3.67	5.52	5.53	5.64
Water absorption (%)	20.68	20.60	18.11	16.73	16.11	15.33	14.60	14.15	12.71
Bulk density (g/cm^3)	1.56	1.59	1.69	1.74	1.71	1.75	1.85	1.87	1.89
Flexural strength (MPa)	1.56	1.94	2.07	0.63	0.60	0.60	1.95	1.86	1.57

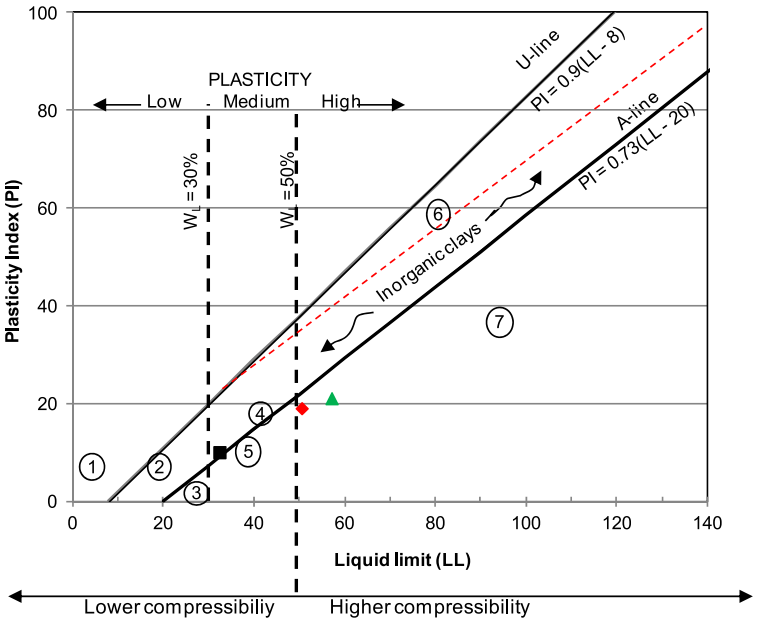

Note: The A-line separates the more claylike materials from silty materials, and the organics from the inorganics.; the U-line indicates the upper bound for general soils.

Fig. 7. Position of Ngaye clays in the Casagrande plasticity chart.

5. Conclusions

The Ngaye alluvial clays were studied for their mineralogy, physicochemistry, and firing properties. The following conclusions are drawn:

1. All layers are composed of kaolinite, quartz, muscovite-illite and smectite as main minerals associated to goethite and anatase.
2. The Winkler diagram indicates that MD10 and MD20 can be used for bricks (common or vertically perforated) formulation. The plasticity after Casagrande chart indicates medium plasticity for MD10 and high plasticity for MD20 and MD30 which allow the manual or the extrusion processability of the samples. It should be quoted that the processability may need addition of fluxing agents and the enrichment in clay content through sifting for sand content reduction.
3. The technological testing of fired products confirms the poor sintering associated to low content in fluxing agents and high sand proportion. To improve the performance of the ceramic products, one may mix the Ngaye alluvial clays with other materials containing sufficient fluxing agents.

Acknowledgements

This work was partially supported by the Geoscience Laboratories (Sudbury, Canada).

Our fieldwork was facilitated by the support of the Cameroon Oil Transportation Company (COTCO).

Lise SALSI of the *Laboratoire Georesources* (Université de Lorraine, France) is greatly acknowledged for her assistance in MEB-EDS analyses.

References

[1] C.M.F. Vieira, R. Sanchez and S.N. Monteiro, Constr. Build. Mater., 22, 781–787 (2008).
[2] M.L. Gualtieri, A.F. Gualtieri, S. Gagliardi, P. Ruffini, R. Ferrari and M. Hanuskova, Appl. Clay Sci., 49, 269–275 (2010).
[3] J. Konta, Appl. Clay Sci., 10, 275–335 (1995).
[4] J. Konta and R.A. Kühnel, Appl. Clay Sci., 11, 273–283 (1997).
[5] C. Nkoumbou, A. Njoya, D. Njopwouo and R. Wandji, in Proceedings of the 1st Conference on the Valorization of Clay Materials in Cameroon and Launching of the Cameroonian Clay Group, Ed. by C. Nkoumbou and D. Njopwouo, April 11–12, Yaoundé, Cameroon (2001) pp. 1–12.
[6] W.A. Allo and H.H. Murray, Appl. Clay Sci., 25, 237–243 (2004).
[7] A. Njoya, C. Nkoumbou, C. Grosbois, C. Njopwouo, D. Njoya, D. Courtin-Nomade, A. Yvon and J.F. Martin, Appl. Clay Sci., 32, 125–140 (2006).
[8] P. Pialy, C. Nkoumbou, F. Villiéras, A. Razafitianamaharav, O. Barres, M. Pelletier, G. Ollivier, I. Bihannic, D. Njopwouo, J. Yvon and J.-P. Bonnet, Clay Miner., 43, 415–435 (2008).
[9] H. Celik, Appl. Clay Sci., 50, 245–254 (2010).
[10] H.H. Murray, Appl. Clay Sci., 17, 207–221 (2000).
[11] H. Tchakoute Kouamo, A. Elimbi, J.A. Mbey, C.J. Ngally Sabouang and D. Njopwouo, Constr. Build. Mater., 35, 960–969 (2012).
[12] H. Tchakoute Kouamo, J.A. Mbey, A. Elimbi, B.B. Kenne Diffo and D. Njopwouo, Ceram. Int., 39, 1613–1621 (2013).
[13] J.A. Mbey, S. Hoppe and F. Thomas, Carbohydr. Polym., 88, 213–222 (2012).
[14] J.A. Mbey, C.J.F. Thomas, Ngally Sabouang, F. Liboum and D. Njopwouo, Appl. Clay Sci., 83–84, 327–335 (2013).
[15] E. Kamseu, C. Leonelli, D.N. Boccaccini, P. Veronesi, P. Miselli, G. Pellacani and U.C. Melo, Ceram. Int., 33, (5) 851–857 (2007).
[16] A. Elimbi and D. Njopwouo, Tile Bricks Int., 18, (6) 364–369 (2002).
[17] J.C. Olivry, Fleuves et rivières du Cameroun, MESRES-Yaoundé-ORSTOM-Paris (1986).
[18] P.-D. Ndjigui, A. Beauvais, S. Fadil-Djenabou and J.P. Ambrosi, J. Afr. Earth Sci., 100, 164–178 (2014).
[19] J. Dirasset, M. Cornachia and R. Dars, Bull. Soc. Géol. France, 7, 101–109 (2000).
[20] A. Le Maréchal and P.M. Vincent, Cah. ORSTOM, Sér. Géol., III, (1) 67–83 (1971).
[21] R. Tchameni, A. Pouclet, J. Penaye, A.A. Ganwa and S.F. Toteu, J. Afr. Earth Sci., 44, 511–529 (2006).
[22] H. Casagrande, Trans. Am. Soc. Civil Eng., 73, 783–811 (1947).
[23] F. Villieras, L.J. Michot, G. Gerard, J.M. Cases and W. Rudzinski, J. Therm. Anal. Calorim., 55, 511–530 (1999).

[24] V.S. Olejnik, L.A.G. Aylmore, A.M. Posner and J.P. Quirk, J. Phys. Chem., 72, (1) 241–249 (1968).
[25] R.L. Frost, E. Makó, J. Kristóf, E. Horváth and J.T. Kloprogge, J. Colloid Interface Sci., 239, 458–466 (2001).
[26] J. Kristof, J. Mink, E. Horvath and M. Gabor, Vibr. Spectrosc., 5, 61–67 (1993).
[27] C.M.F. Vieira, R. Sanchez and S. Monteiro, Constr. Build. Mater., 22, 781–787 (2008).
[28] S. Mahmoudi, E. Srara and F. Zargouni, Appl. Clay Sci., 42, 125–129 (2008).
[29] C. Melo, E. Kamseu and C. Djangang, in Proceedings of the 1st Conference on the Valorization of Clay Materials in Cameroon and Launching of the Cameroonian Clay Group, Ed. by C. Nkoumbou and D. Njopwouo, April 11–12, Yaoundé, Cameroon (2001) pp. 57–69.
[30] E.D. Quesada, M.C. Garcia, M.M.L. Cartas, C.M.T. Palomino, P.L. Villarego, C.N. Perez and C.A.F. Iglesias, Appl. Clay Sci., 52, 270–276 (2001).
[31] B.K. Ngun, H. Mohamad, S.K. Sulaiman, K. Okada and Z.A. Ahmad, Appl. Clay Sci., 53, 33–41 (2011).